Journal of The Electrochemical Society

The Electrochemical Society
Advancing solid state & electrochemical science & technology

ACCEPTED MANUSCRIPT

Laccase Polyphenolic Biosensor Supported on MnO2@GNP Decorated SPCE: Preparation, Characterization, and Analytical Application

To cite this article before publication: Sladjana Djurdjic *et al* 2021 *J. Electrochem. Soc.* in press https://doi.org/10.1149/1945-7111/abeaf2

Laccase Polyphenolic Biosensor Supported on MnO2@GNP Decorated SPCE: Preparation, Characterization, and Analytical Application

Journal:	*Journal of The Electrochemical Society*
Manuscript ID	JES-102937.R2
Manuscript Type:	Research Paper
Date Submitted by the Author:	26-Feb-2021
Complete List of Authors:	Djurdjic, Sladjana; University of Belgrade Faculty of Chemistry, Vukojević, Vesna; Institute of Chemistry Technology and Metallurgy, Institute of Chemistry Vlahović, Filip; University of Belgrade Faculty of Chemistry Ognjanović, Miloš; VINCA Institute of Nuclear Sciences, Department of Theoretical Physics and Condensed Matter Physics Kalcher, Kurt; Karl-Franzens-Universitat Graz Ćirković Veličković, Tanja; University of Belgrade Faculty of Chemistry Mutić, Jelena; University of Belgrade Faculty of Chemistry Stanković, Dalibor; Univerzitet u Beogradu Hemijski fakultet, ; VINCA Institute of Nuclear Sciences,
Keywords:	Electroanalytical Electrochemistry, Graphene, Nanoscale materials, Bioelectrochemistry

Laccase Polyphenolic Biosensor Supported on MnO_2@GNP Decorated SPCE: Preparation, Characterization, and Analytical Application

S. Đurđić,[1,z] V. Stanković,[2] F. Vlahović,[3] M. Ognjanović,[4] K. Kalcher,[5] T. Ćirković Veličković,[1,6,7,8] J. Mutić,[1,6] and D. M. Stanković,[1,9,z]

[1]University of Belgrade - Faculty of Chemistry, 11000 Belgrade, Serbia

[2]Institute of Chemistry, Technology and Metallurgy, University of Belgrade, 11000 Belgrade, Serbia

[3]Innovation center of the Faculty of Chemistry, University of Belgrade, 11158 Belgrade, Serbia

[4] Department of Theoretical Physics and Condensed Matter Physics, „VINČA" Institute of Nuclear Sciences - National Institute of the Republic of Serbia, University of Belgrade, Belgrade, Serbia

[5]Institute of Chemistry - Analytical Chemistry, Karl-Franzens University Graz, A-8010 Graz, Austria

[6]Ghent University Global Campus, Incheon, South Korea

[7]University of Belgrade - Faculty of Chemistry, Centre of Excellence for Molecular Food Sciences

[8]Serbian Academy of Sciences and Arts, Belgrade, Serbia

[9]Department of Radioisotopes, "Vinča" Institute of Nuclear Sciences - National Institute of the Republic of Serbia, University of Belgrade, Belgrade, Serbia

[z]E-mail: sladjanadj@chem.bg.ac.rs; dalibors@chem.bg.ac.rs

Abstract

Based on graphene nanoplatelets capability to build block composites, as well as well-known electrochemical characteristic of the manganese oxide materials, in the present research, a nanocomposite, formed from graphene nanoplatelets (GNP) and manganese(IV)-oxide (MnO_2) nanoparticles, has been proposed as a novel and convenient support for enzyme immobilization. Performance of screen printed carbon electrodes (SPCEs) was significantly improved after their modification with GNP@MnO_2 (SPCE/GNP@MnO_2). The polyphenolic index biosensor was prepared by applying the drop coating technique using laccase and Nafion®. Developed biosensor shows a fast and reliable amperometric response toward caffeic acid, as a model compound, at operating potential of +0.40 V (vs. Ag/AgCl), with a wide linear range and detection limit of 1.9 μmol L^{-1}. Developed procedure was successfully applied for the determination of polyphenolic indexes in wine samples. Recovery tests indicate excellent accuracy and precision of the method, concluding that the biosensor can offer a fast, accurate, reliable and precise determination of the polyphenolic index. More importantly, our results suggest a great potential for the application in real samples.

Introduction

Polyphenols are considered as one of the most important natural antioxidants. Phenolic compounds represent secondary metabolites generated in various important biochemical processes of plant metabolism.[1] They play an essential role in the removal of free radicals, obtained by oxidative processes in the organism. Antioxidant activity is closely related to the prevention of various diseases, such as stroke, heart attack, diabetes and cancer. In addition to their antioxidant ability, polyphenols can exhibit other biological properties, such as antibacterial, antiviral, antimicrobial and anti-inflammatory activity.

Food products represent one of the main sources of polyphenolic compounds. Regular consumption of fruits (apples, grapes, black currants, citrus fruits), vegetables (tomatoes, cabbage, onions)[2] and spices (rosemary, sage)[3] contribute to proposed polyphenols average intake of 1g/day.[4] High polyphenolic content is present in beverages such as tea, coffee, fruit juice and especially wine.[2,5] Since polyphenols are one of the most abundant soluble chemical species present in wines, they exhibit a high absorption ratio and considerable bioavailability.[6] For all these reasons, polyphenols, present in wines, are the topic of great number of scientific researches.[6,7]

A number of highly sensitive and reliable analytical methods were utilized for the determination of polyphenolic composition. Separation of different polyphenolic species can be obtained by various analytical methods, such as high performance liquid chromatography (HPLC), gas chromatography (GC) or capillary electrophoresis (equipped with subsequent UV or mass detection),[8,9] while the total polyphenolic composition (total polyphenolic index) can be determined using standard spectrophotometric Folin-Ciocalteu method.[7] However, these methods require long sample preparation, expensive equipment and skilled personnel.[8,10] On the other hand, electrochemical techniques, especially voltammetric and amperometric methods, offer a number of advantages such as simplicity, time saving, low cost, easy sample preparation and low consumption of reagents, when compared to other analytical methods.[6,10] Therefore, electroanalytical methods are most commonly used for the detection of various metallic ions, pharmaceuticals and especially biologically important compounds.[11-17]

Electrochemical biosensors have proven to be an inexpensive, but highly efficient analytical tool for the detection of polyphenols in clinical diagnostics, food and environmental quality assessment, as well as in industrial and pharmaceutical analysis.[8-10,18,19] Enzymes, which are essential for successful construction of amperometric biosensors (applicable for the detection and determination of polyphenols), are in most cases laccase, tyrosinase and peroxidase.[10,19] Laccase can be obtained from certain fungi, bacteria or plants and belongs to the family of multicopper oxidases. This enzyme catalyzes the oxidation of aromatic compounds (polyphenols, anilines, lignins) with a simultaneous reduction of molecular oxygen to water.[20] Most importantly, laccase does not require the presence of cofactors, such as H_2O_2, and therefore it represents the most suitable enzyme for polyphenolic detection in various analytical systems.[9,19]

Screen printed carbon electrodes (SPCEs), especially in recent years, are widely used for the construction of disposable electrochemical sensors and biosensors.[21,22] Appropriate conductive ink was used for the production of SPCEs.[23] Practical preparation of these electrodes is simple, and most importantly they can be considered as a relatively cheap tool for

electrochemical detection. Besides the fact that SPCEs can be applied in a wide potential window, they are characterized by excellent electron transfer reactivity, low background current and excellent reproducibility of performed experiments. For all these reasons, SPCEs are most commonly used as working electrodes in electrochemical determinations.

Graphene has found enormous application in the fields of energy storage and conversion, thermal conductivity, supercapacitors, electronic and optical devices, as well as environmental remediation.[24-34] In addition to applications in industry and technology, graphene-based materials have a leading role in chemical, physical and mechanical research. In the field of electroanalysis, the greatest advantage of graphene is reflected in energy storage and sensing.[35,36] Graphene is a two-dimensional sheet of sp^2 bonded carbon atoms in hexagonal configuration. This configuration of graphene provides high mechanical strength, thermal conductivity and sufficient surface area.[35-37] Biological substrates can be immobilized on the electrode surfaces using several approaches.[38-45] Various studies have shown that graphene nanomaterials represent a suitable base for enzyme immobilization.[21,22,37,46-48] In addition, these nanomaterials strongly influence the kinetic rate of electron transfer for many different electroactive species.[22] Graphene nanoplatelets (GNP), also known as graphene nanosheets, are graphene derivatives which consist of 10-100 graphene layers, with a thickness of ~3-30 nm.[36,49] GNP are characterized by large surface area, high conductivity, remarkable electrocatalytic activity, high sensitivity and low cost. GNP could be used as building blocks to construct composites with negative electromagnetic parameters, which has potential applications for electronic devices. In combination with superior electrochemical characteristics of manganese oxide nanoparticles, this can be a promising pathway in this field of research.[50] Due to these excellent electrochemical properties, graphene nanomaterials hold great potential for the construction of electrochemical sensors and biosensors.[49,51-53]

In addition to graphene nanomaterials, great attention has been paid to metal oxide nanoparticles (MONp) and their application in scientific research and technological processes.[54,55] MONp are characterized by unique magnetic and electronic properties. Due to their considerable electrocatalytic activity, MONp have found their irreplaceable application in the field of electroanalysis.[56,57] Manganese(IV)-oxide (MnO_2) nanoparticles represent one of the most attractive nanomaterials suitable for electrode modification and tuning of their electrochemical properties. Although this material is appreciated for its basic properties, like low-cost and non-toxicity, it is of utmost importance to highlight that MnO_2 nanoparticles as a modification agent can greatly enhance sensitivity and selectivity of electrochemical sensors and biosensors.[21,58-61]

Polyphenolic index determination using electrochemical method is nowadays widely used, taking into account simplicity of the method, cheap and easy manipulated equipment and no sample preparation request. Lugonja and co-workers[62] studied practical application of electrochemical methods for the monitoring of milk quality regarding polyphenolic index estimation using cyclic voltammetry and differential pulse methods. In this study, authors confirmed that both electrochemical methods possess high complementarity with standard spectrophotometric methods, and that can be used for this purpose. Similarly, Blasco and co-workers[63] studied potential application of electrochemical methods for polyphenolic index determination *vs.* standard spectrophotometric methods. In addition, authors indicates that caffeic acid is most suitable standard for development of the electroanalytical method.

According to this study[63], there is constant need for the improvement of the electrochemical methods, dominantly regarding novel electrode systems, which will overcome some lack of, nowadays, most used glassy carbon electrode, such as high adsorption at the surface of phenolic compounds and to improve limit of detections of electrochemical methods.

In present work, we describe the development of electrochemical biosensor, convenient for polyphenol monitoring. To the best of our knowledge, this is the first work that shows how to modify GNP with MnO_2 nanoparticles (GNP@MnO_2) and develop a biosensor, suitable for the determination of polyphenol index. GNP@MnO_2 nanocomposite was simply prepared and characterized by SEM and XRD techniques. Thereafter, SPCEs were modified with GNP@MnO_2 composite (SPCE/GNP@MnO_2). In order to obtain the biosensor, surface of SPCE/GNP@MnO_2 electrode was modified with enzyme laccase (from *TrametesVersicolor* (TvL)) and later with Nafion (SPCE/GNP@MnO_2/TvL/Naf), using the drop coating technique.

Experimental

Reagents and solutions - All chemicals used in this study were of analytical grade. Ultra-pure water prepared by Millipore Simplicity 185 System (incorporating dual UV filters, 185 and 254 nm) was used for the preparation of all aqueous solutions. Graphene nanoplatelets (thickness 2-10 nm, diameter 2~7μm) were supplied by ACS Material (Pasadena, California). Fungal laccase from *Trametes Versicolor* (benzenediol: oxygenoxidoreductase EC1.10.3.2, activity provided on the bottle >10 U/mg) was supplied by Sigma Aldrich (USA) and stored at -18°C.

Manganese (II) nitrate tetrahydrate and potassium permanganate (used for MnO_2 nanoparticles preparation), caffeic acid (used as model analyte), potassium ferricyanide, $K_3[Fe(CN)_6]$ and potassium ferrocyanide, $K_4[Fe(CN)_6]$ (used for reversibility examination of the system) were supplied by Merck (Germany).

Three supporting electrolytes were used in this study. Sodium acetate and acetic acid (17 mol L^{-1}) were used for the preparation of 0.1 mol L^{-1} acetate buffer (AcB) solution. Britton Robinson buffer (BRB) solution was prepared by dissolving 2.80 mL of phosphoric acid (16 mol L^{-1}), 2.40 mL of acetic acid (17 mol L^{-1}) and 2.48 g of boric acid in 1 L of ultra-pure water. Dibasic sodium phosphate (Na_2HPO_4) and monobasic sodium phosphate (NaH_2PO_4) were used for the preparation of 0.1 mol L^{-1} phosphate buffer (PB) solution. All of the previously listed substances were also supplied by Merck (Germany).

N,*N*-Dimethylformamide, DMF (used for the preparation of nanocomposite suspensions) and interfering substances (see section *Interferences study*) were supplied by Alfa Aesar (Germany). Both red and white wine were purchased at a local market.

Instrumentation - Crystallographic properties of the initial material were examined by the X-ray powder-diffraction (XRPD) performed on a high-resolution Smart Lab® X-ray diffractometer (Rigaku, Japan) using Cu Kα radiation (λ = 0.1542 nm). The data were collected in the 2θ range from 10° to 70° in steps of 0.02° and with the exposition of 2 sec per step operated at 40 kV and 30 mA. Morphology of synthesized samples were investigated using a field emission-scanning electron microscope FE-SEM MIRA3 (Tescan, Czech Republic), coupled with EDS analyzer (Oxford, UK) operating at 30 kV. The sample was prepared by placing a drop of particles suspended in water onto a carbon-coated copper grid, while allowing them to dry at RT for FE-SEM observations. The micrographs were analyzed manually by

Image J software. The mean particle size and distribution were evaluated by measuring the largest internal dimension of 100 nanoparticles and collected data were fitted to a log-normal function, $y = y_0 + \frac{A}{\sqrt{2\pi}\omega x}\exp\frac{-\left[\ln\frac{x}{x_c}\right]^2}{2\omega^2}$. Mean diameter size, as well as index of polydispersity (PdI) were obtained.

The cyclic voltammetry and chronoamperometry measurements were carried out using a potentiostat PalmSens 3 (PalmSens BV, The Netherlands), equipped with PST Trace 5 software. The conventional three-electrode system (total volume of 25 mL) was established using SPCEs as working electrodes, Ag/AgCl/3 mol L^{-1}KCl as reference electrode and Pt wire (diameter 0.5 mm) as the counter electrode. For all pH measurements, a pH meter (model Orion 1230) equipped with a combined glass electrode (model Orion 9165BNWP) was used.

Preparation of SPCE -Carbon ink (No. C50905DI, Gwent, Pontypool, UK) was used for the preparation of SPCEs. A thick layer of carbon ink was applied to the ceramic supports with a laser pre-engraved template (thickness 100 mm, electrode printing area 105mm^2, No. CLS 641000396R, Coors Ceramics GmbH, Chattanooga, TN, USA). Using a screen-printing device, the layer of applied thick ink was evenly distributed. Printed electrodes, generated using this procedure, were dried at room temperature. After 24 h, the SPCEs were ready and operational for further experiments.

Preparation of GNP@MnO_2 nanocomposite -Synthesis of GNP@MnO_2 nanocomposite was carried out following the procedures reported in the literature.[21,64] In the first step, 10 mg of GNP was suspended in 5 mL of ultra-pure water and ultra-sonicated for 1 h. The final concentration of GNP composite was 2 mg mL^{-1}. The second step was based on the dissolution of 21.8 mg of manganese (II) nitrate tetrahydrate in 20 mL of ultra-pure water. These two solutions were then mixed together and after 2 h of ultra-sonication, a uniform brown suspension was formed. Finally, 45.7 mg of $KMnO_4$ was dissolved in 25 mL of ultra-pure water and added in GNP-$Mn(NO_3)_2$ suspension. After 6 h of magnetic stirring, the obtained GNP@MnO_2 nanocomposite was centrifugated and washed three times with ultra-pure water, then with ethanol and finally dried at 25°C overnight. MnO_2 nanoparticles were prepared following the same procedure, only without the addition of the GNP. Then, GNP@MnO_2 nanocomposite, GNP and MnO_2 nanoparticles were suspended in DMF and the final concentration of every suspension in the resulting mixture was 2 mg mL^{-1}.

Preparation of working electrodes and biosensor - The surface of SPCE was modified with 5 µL of GNP@MnO_2 nanocomposite and allowed to dry overnight (SPCE/GNP@MnO_2). In order to compare the electrochemical performance of the obtained nanomaterials, the SPCEs were modified with 5 µL of MnO_2 nanoparticles (SPCE/MnO_2) and 5 µL of GNP (SPCE/GNP). For the preparation of laccase solution (TvL), 0.1 g of enzyme was dissolved in 10 mL of PB (pH=7.40) and obtained solution was kept in refrigerator until use. On the surface of SPCE/GNP@MnO_2, 5 µL of laccase solution was applied and dried at 4°C one day. The surface of the electrode, modified in this way, was further covered with 2.5 µL of Nafion (0.5 % in ethanol). Obtained biosensor (SPCE/GNP@MnO_2/TvL/Naf) was dried 2 hours at 4°C and used for electrochemical measurements.

Results and Discussion

Electrode surface characterization by FE-SEM and XRPD methods - Structure and

morphology of pure MnO_2, GNP and MnO_2/GNP nanocomposite (characterized by FE-SEM) are presented in Figure 1. As illustrated (Figure 1A), MnO_2 nanoparticles were spherical in shape, stacked densely on each other, with an average diameter of about 153 ± 2 nm. Obtained nanoparticles undergo a log-normal size distribution with PdI at 8.4% (Inset of Figure 1A). As it can be seen from Figure 1B, the GNPs are quite thin, with a smooth surface, yet certain nanoplatelet sheets were aggregated and corrugated, with a diameter of 2-4 μm. GNPs were flat, transparent and with no additional substances adhered to the surface. Finally, as can be observed from Figure 1C, ball-like MnO_2 nanoparticles were randomly deposited and tightly bonded to the surfaces of nanoplatelets, acting as spacers which keep the neighboring sheets separated. All these structural factors lead to a wrapped and corrugated morphology of GNP@MnO_2 composite. Such a unique morphology will provide more physical bonding points between nanoparticles and GNPs. Newly formed wrinkles, present on the surface of the GNPs, are considered as aggregation prevention for GNPs. Moreover, this morphological aspect is important for maintaining a high surface area, which is crucial for the electron transfer rate and good conductivity. Successful decoration of graphene nanoplatelets was also confirmed after EDS mapping analysis (Figure S1).

The diffraction patterns of MnO_2 nanoparticles, GNP and GNP@MnO_2 nanocomposite are presented in Figure 2. The XRPD profile of MnO_2 (blue line) resulted with characteristic diffraction peaks of 12.8°, 18.2°, 28.8°, 37.7°, 42.4°, 50.0° 56.4° and 60.2° at 2θ, which can be assigned to (110), (200), (310), (211), (301), (411), (600) and (521) crystal planes of α-MnO_2, respectively (JCPDS card #44-0141).[65] The diffraction pattern of GNP (green line) showed a sharp peak of 25.9° at 2θ, corresponding to the interlayer spacing of 0.344 nm, based on Bragg's law. This was attributed to the high crystallinity (002) of GNPs. The peaks at 42.2°, 44.0° and 53.7º correspond to the reflection of (100), (101) and (004) planes, confirming that graphene nanoplatelets were not completely exfoliated.[66] Consequently, the XRPD pattern of GNP@MnO_2 (purple line) points out to the successful formation of composite material, with all of the characteristic diffraction peaks for MnO_2 and GNP still preserved.

Cyclic voltammetry study

Electrochemical behavior of working electrodes - Electrochemical behavior of unmodified SPCE and modified SPCEs (SPCE/GNP, SPCE/MnO_2 and SPCE/GNP@MnO_2) was examined by a cyclic voltammetry in the presence of the 0.5 mmol L^{-1} $K_3[Fe(CN)_6]/K_4[Fe(CN)_6]$ in 0.1 mol L^{-1} PB (pH=6.50) with a scan rate of 50 mV s^{-1} (Figure 3A). Applied potential was held in the range from -0.5 V to +1.0 V. The cathodic to anodic current (I_{pa}/I_{pc}) ratio was found to be around 1.0, for all four working electrodes, implying that the process is reversible. However, this is not supported by the fact that the differences in peak potentials (ΔEp), which are higher than 59 mV. It is noticeable that SPCE/MnO_2 electrode shows the lowest current intensity for this system, while the significant differences between unmodified SPCE and SPCE/GNP were not discerned. Decrease in these currents can be attributed to the repulsive forces between the surface hydroxyls on SPCE/MnO_2 and the negatively charged $K_3[Fe(CN)_6]$ that is used as a model in this study, while on using the caffeic acid under study this electrode shows better results due to the better electrochemical performances and higher electron transfer rate (Figure 3B). On the other hand, SPCE/GNP@MnO_2 electrode provides the best electrochemical characteristics, i.e. the highest current intensities and well defined and sharp oxidation and reduction peaks. It is obvious that

peak separation potential in this case was bigger than using commercial electrodes. According to the literature and our own experience this is expected behaviour for used electrochemical system. Compared to homogeneous carbon electrodes (e.g. glassy carbon electrode), SPCE often exhibits slower electron transfer, since heterogeneous carbon materials are used for their construction. In addition, the composition and thickness of the printed layer directly affect the resistance of the electrode. All these factors together enhance the most important properties of the electrode, leading to higher background currents and wider peak separation even in cases of reversible processes, which is very well documented in numerous papers.[67,68] Finally, it can be concluded that electrochemical characteristics, such as electrical conductivity, effective surface area and diffusion layer, were significantly improved due to the synergistic effect of MnO_2 and GNP combination.

Possible reversibility of the system was tested with the investigation of the electrochemical response of the unmodified SPCE and modified SPCE with GNP@MnO2 nanocomposite in solution containing 0.5 mmol L^{-1} $K_3[Fe(CN)_6]/K_4[Fe(CN)_6]$ in 0.1 mol L^{-1} PB (pH=6.50). Results are given in Figure S2. With the increase of the scan rate linear shifts of the anodic peak to more positive value and cathodic peak to more negative value with constant value of ΔE. These measurements indicate that electrode reaction at the surface is rather irreversible. Using this data, active surface area of working electrodes was calculated according to the Randles-Sevcik equation[69]. Active surface area for bare SPCE and SPCE/GNP@MnO_2 were 182 mm^2 and 400 mm^2, respectively, indicating significant increase in the effective surface of the SPCE after modification with the target nanocomposite.

In addition, under the same instrumental and experimental conditions, the electrochemical responses of the working electrodes in the presence of 0.1 mmol L^{-1} caffeic acid were examined. As it can be clearly seen from Figure 3B, SPCE modified with our composite (SPCE/GNP@MnO_2) provides the highest current intensity, as well as much better defined, sharp redox peaks, if compared to other SPCEs. As in the previous case, we can conclude that the combination of these two highly promising electrode modification materials (GNP and MnO_2 nanoparticles) significantly influenced and considerably improvement electrochemical characteristics of the screen printed carbon electrodes.

Since for the cyclic voltammetry experiment, the composite SPCE/GNP@MnO_2 shows good electrochemical characteristics toward caffeic acid (Figure 3B), amperometric behavior of SPCE working electrodes and the biosensor was tested, in order to determine the best possible electrochemical performance. The chronoamperometric response was followed by adding caffeic acid in a concentration range from 0.04 mmol L^{-1} to 0.15 mmol L^{-1} in 0.1 mol L^{-1} AcB (pH= 4.60), at the working potential of 0.4 V, under stirring conditions. Figure S3B shows that the developed biosensor, under optimized experimental and instrumental conditions, provides the best amperometric performance, i.e., the highest current intensity and the most stable current signal. Thus, further method optimization was done using this biosensor as working platform.

pH influence of the supporting electrolyte on the biosensor performances - According to the data find in the literature, laccase shows the highest activity in the pH range from 4 to 5.[70-73] For the investigation of biosensor performance, in this study, 0.1 mol L^{-1} AcB and 0.1 mol L^{-1} BRB were used as supporting electrolytes. Electrochemical responses of biosensor for both supporting electrolytes were followed by cyclic voltammetry in presence of 0.3 mmol L^{-1}

caffeic acid in a potential window in the range from -0.5 V to +1.0 V (scan rate 50 mV). AcB and BRB were applied in pH range from 4.00 to 5.30. AcB (pH=4.60) provides higher current intensity and better definition of obtained peaks, if compared to the same pH of the BRB (Figure S4). Figure S4A suggests that there is no significant difference in the current intensities between pH=4.30 and pH=4.60 but, yet pH=4.60 gives a sharper and better defined shape for both peaks. For this reason, the AcB (pH=4.60) was selected as the supporting electrolyte for all further measurements.

Hydrodynamic chronoamperometric measurements by SPCE/GNP@MnO_2/TvL/Naf biosensor

Optimization of working potential - Optimization of working potential plays an important role during the amperometric measurements which employ electrochemical biosensors. Namely, it is important to apply the lowest possible potential, at which the biosensor shows good performance, since at higher potentials other electrochemically active species can undergo an ox/red processes. On the other hand, the increase in the working potential affects the current intensity, which leads to a significant change in the limit of quantification (LOQ) and limit of detection (LOD). In order to reduce the impact of interfering substances at higher working potentials, mediators or, in the last few years, nanomaterials are included in rational design of biosensors.[74,75] Influence of different working potentials on the electrochemical response of our biosensor was tested by adding successive aliquots of caffeic acid to 0.1 mmol L^{-1} AcB (pH=4.60), under stirring conditions. Concentration range of caffeic acid was from 0.04 mmol L^{-1} to 0.20 mmol L^{-1}. Working potential was applied in the range from 0.3 V to 0.5 V. As can be noted from Figure S3A, working potential of 0.4 V provides the highest current and the most stable signal. Most importantly, further increase of working potential does not significantly affect the amperometric response, and therefore the working potential of 0.4 V was chosen as optimal for all further measurements.

Analytical characterization of the fabricated biosensor - The laccase reaction in the biosensing process includes the oxidation of the enzyme molecule by an oxidizing agent using molecular oxygen under ambient conditions. Re-reduction process happens at the enzyme molecules to its native form by electrons received from the phenolic compound. After that, the phenoxy radical or quinine produced from the enzymatic reaction is re-reduced at the surface of the electrode, which results in a proportional current to the concentration of phenolic compound.[76] The amperometric response of SPCE/GNP@MnO_2/TvL/Naf biosensor toward the substrate, caffeic acid, was examined by hydrodynamic chronoamperometry. Different aliquots of 5 mmol L^{-1} caffeic acid were added consecutively in 20 mL of AcB (pH=4.60) with continuous stirring. The current intensity of the biosensor was followed as a function of time, at the optimized working potential of 0.4 V (Figure 4). The obtained current response was plotted against the concentration of caffeic acid and corresponding dependence can be found in the inset of Figure 4. Linear concentration range for caffeic acid, obtained with developed biosensor, was from 5 µmol L^{-1} to 0.32 mmol L^{-1}. The linear regression equation can be expressed as $I(A) = 1.65 \times 10^{-7} + 4.48 \times 10^{-6}$ C (mmol L^{-1}), with r^2=0.9996. LOD and LOQ were calculated from the calibration curve as $3S_{y/x}$/slope and $10S_{y/x}$/slope, respectively, where is: $S_{y/x}$ - standard error of estimate, *b* - slope of the regression line. LOD and LOQ were found to be 1.9 µmol L^{-1} and 5.8 µmol L^{-1}, respectively. Essential electroanalytic parameters, such as working potential, linear concentration range, LOD and sensitivity of the developed

SPCE/GNP@MnO_2/TvL/Naf biosensor, were compared with other laccase biosensors reported in the literature. Table 1. shows that the developed polyphenolic biosensor provided a wide linear concentration range compared to previous reports. Also, the SPCE/GNP@MnO_2/TvL/Naf biosensor offer high sensitivity during quantification of caffeic acid with the proposed amperometric method. Such specific biosensor properties can be addressed to high affinity of the immobilized enzyme for caffeic acid, as well as, to efficient immobilization of laccase for SPCE/GNP@MnO_2 matrix. The synthesis procedure of the proposed nanocomposite is quite simple and does not require a long period of preparation. In addition, the preparation of the biosensor itself was performed in two very simply steps. On the other hand, the developed polyphenolic biosensor shows a relatively higher LOD toward caffeic acid. However, as polyphenols are found to be present in significant amount in food samples and beverages, the LOD of the proposed polyphenolic biosensor is sufficient for their detection.

Storage stability, repeatability and reproducibility studies - Another important property of SPCE/GNP@MnO_2/TvL/Naf biosensor studied in the present research was the storage capacity. After constant use of biosensors during the day (n=15), the loss of biosensor activity did not exceed 7%. After the measurements were successfully completed, the biosensor was stored at +4 °C overnight. Remaining biosensor activity was investigated after 2, 5 and 7 days, whereby the biosensor activity decreased to 91.6 %, 87.8 % and 77.1 %, respectively. It is important to mention that the biosensor successfully detects caffeic acid after the mentioned test period. Since SPCEs are usually used as disposables, and designed for a small number of measurements, it is important to highlight that our SPCE/GNP@MnO_2/TvL/Naf biosensor shows satisfactory analytical properties, such as precision and accuracy, for multiple measurements within a period of 5 days.

The repeatability of the developed biosensor was tested by measuring three different concentrations in five consecutive measurements. Relative standard deviations (RSDs) for concentrations 7 μmol L^{-1}, 50 μmol L^{-1} and 210 μmol L^{-1} were 2.94 %, 2.07 % and 1.84 %, respectively. These results indicate excellent repeatability of developed SPCE/GNP@MnO_2/TvL/Naf biosensor and the proposed method.

The reproducibility of the developed biosensor was examined by measuring 70 μmol L^{-1} of caffeic acid with ten independently prepared biosensors. Concentrations were calculated from the calibration curve. RSD of 3.97 % indicates excellent reproducibility of the proposed preparation procedure for the fabrication of SPCE/GNP@MnO_2/TvL/Naf biosensor.

All obtained results considered together, lead us to an important conclusion that the selection and application of proposed, highly promising materials, play an essential role in the construction of an efficient biosensor. In addition, optimization of the polyphenolic detection method using the SPCE/GNP@MnO_2/TvL/Naf significantly improves electroanalytical parameters, such as linear working range, limit of detection, repeatability, reproducibility, accuracy and precision, as well as the stability and life-time of the biosensor.

Interferences study - Selectivity of developed SPCE/GNP@MnO_2/TvL/Naf biosensor and the proposed electrochemical procedure was examined by monitoring the effect of possible interfering substances. Amperometric response of developed SPCE/GNP@MnO_2/TvL/Naf biosensor toward caffeic acid (20 μmol L^{-1}) was followed, under optimized experimental and instrumental conditions, by successive addition of glucose (Glu), fructose (Fru), ascorbic acid

(Asc), tartaric acid (Tart), uric acid (Uric), paracetamol (Par), *p*-nitrophenol (*p*-nPh) and dopamine (Dop). Glu and Fru were applied at a concentration of 20 μmol L^{-1}, while the concentrations of other substances were 10 μmol L^{-1}. Figure S5 indicates that the quantification of caffeic acid, using proposed biosensor, is affected by dopamine, while negligible changes in the current signal were recorded by the addition of other compounds. The increase in the current signal (up to 30 %), in the case of dopamine, can be explained by possible tendency of this chemical species to be oxidized at selected working potential.

Also, the selectivity of the developed biosensor towards metal ions was examined. K^+, Na^+, Mg^{2+}, Ca^{2+} and Fe^{3+} were applied at a concentration of 0.5 mmol L^{-1}, while 20 μmol L^{-1} was the concentration of Cu^{2+}, Pb^{2+} and Cd^{2+}. These ions were chosen because of their presence in water, as well as food and beverages. The amperometric response of the developed biosensor to 20 μmol L^{-1} caffeic acid, in the presence of the mentioned metal ions, was monitored under optimized experimental and instrumental conditions. The results showed that metal ions do not affect the quantitative determination of caffeic acid using the developed biosensor and the proposed amperometric method. This can be attributed to the activity of the biosensor at positive potential, while metal ions are mostly electroactive at lower or negative potentials.

Based on the results obtained for selectivity, it can be concluded that developed SPCE/GNP@MnO_2/TvL/Naf biosensor, in combination with the proposed optimized method, can be used for quantification of polyphenol compounds in food and beverages, since chemical compounds (sugars and vitamins), as well as metallic ions have negligible interference. Additionally, MnO_2 nanoparticles can lover the influence of interferences.[74] For all these reasons, the developed biosensor can be considered as a convenient tool for analysis of blood serum and urine samples (clinical samples), since it has been proven that compounds present in these biological fluids have minimal matrix effect. It is important to keep in mind that dopamine levels must be defined in advance.

Finally, there are several approaches for further improvement of the biosensors electrochemical performance, such as modification of the electrode surface with nanocomposites, as well as successful and fast immobilization of a specific enzyme to the nanocomposite surface. Improving the bonding of the nanocomposite to the electrode surface can be achieved by adjustment and modification of existing core-shell preparation procedures, as well as by considering the EDC/NHS reaction mechanism and nanomaterial structure. Than, rational application of chemical reactions and resulting modifications of the nanocomposites, as well as adaptation of the enzyme can significantly increase the immobilization rate of the enzyme. Application of such approaches will result in higher effective activity of the biosensor, as well as higher long-term stability and selectivity.

Application to wine samples. Validation of method by glassy carbon electrode - Possibility for application of developed SPCE/GNP@MnO_2/TvL/Naf biosensor, in combination with the proposed method, for the examination of real samples was investigated. The bioelectrochemical polyphenolic index (BPI) was analyzed in commercial red and white wine (11-12%, v/v). Standard addition method was used for quantification of polyphenol content in wine samples. Volume of 100 μL of red wine was added to 20 mL of 0.1 mol L^{-1} AcB (pH=4.60). Using developed biosensor, under optimized conditions, the current intensity was recorded after five successive additions of 100 μL of 5 mmol L^{-1} caffeic acid. Following the same procedure, the electrochemical response of biosensor was monitored after the

successive addition of 5 mmol L^{-1} caffeic acid of 150 µL and 200 µL, respectively. The same experimental steps were used to determine BPI in white wines. Results were extracted from the calibration curve and the concentrations were expressed as *mg* caffeic acid equivalents per *L* of wine (Table 2).

In order to validate the proposed method, electrochemical polyphenolic index (EPI) in wine samples was determined by glassy carbon electrode. According to the literature data, glassy carbon electrode is the most frequently used electrode for electrochemical determination of polyphenolic index (antioxidant activity).[83,84] Therefore, glassy carbon electrode was used as the standard, in order to validate the proposed method with the developed biosensor. Experimental procedure was similar to the one used for the determination of polyphenolic index using developed biosensor: 100 µL of wine samples were spiked with different standard additions of 5 mmol L^{-1} caffeic acid and the electrochemical response of glassy carbon electrode was monitored. As can be seen in Table 2., the values obtained during the determination of polyphenolic index, by utilizing the developed biosensor, are in good agreement with the values obtained using the glassy carbon electrode. Recovery tests show that developed SPCE/GNP@MnO_2/TvL/Naf biosensor, in combination with the proposed method, provide high accuracy and precision during the determination of polyphenolic index in real samples, with minimal influence of the matrix effects.

Conclusions

In the present research, we have demonstrated that modification of SPCE with GNP@MnO_2 composite (SPCE/GNP@MnO_2) tunes and ensures excellent electrochemical performance of resulting biosensor, which can be further used for the analysis of the polyphenolic index. Laccase from *Trametes Versicolor* (TvL) was successfully immobilized, by drop coating method, at the surface of SPCE/GNP@MnO_2. Finally obtained SPCE/GNP@MnO_2/TvL/Naf biosensor exhibited a wide linear range for caffeic acid detection (5 µmol L^{-1} to 0.32 mmol L^{-1}) with a LOD of 2.1 µmol L^{-1} and sensitivity of 455 nA/µmol L^{-1}. Moreover, the developed biosensor shoved excellent stability, repeatability and reproducibility for the determination of caffeic acid. Additionally, the influence of possible interfering substances on the electrochemical response of the biosensor was investigated. SPCE/GNP@MnO_2/TvL/Naf biosensor was employed for the determination of polyphenolic index in red and white wines. The developed method was validated using a glassy carbon electrode. Recovery values indicate that the developed biosensor provides high accuracy and precision during the determination of the polyphenolic index in wines. The stability of the electrode surface, together with easy preparation, long-term usage and reproducible procedure are offering great opportunities for potential manufacturability of the proposed biosensor.

Acknowledgments

This work was funded by the Ministry of Education, Science and Technology, the Republic of Serbia, Contract number: 451-03-68/2020-14/200168 and Eureka project call, E! 13303 MED-BIO-TEST.

References

1. L. Jakobek, *FoodChem.*, **175**, 556 (2009).
2. E. Cieślik, A. Gręda andW. Adamus, *Food Chem.*, **94**, 135(2006).
3. Y. Li, H. Liu, Q. Han, B. Kong and Q. Liu, *Food Chem.*, **222**, 74 (2017).
4. A. Scalbert and G. Williamson, *J Nutr.*, **130**, 2073S (2000).
5. J. G. Bordonaba and L.A. Terry, *Talanta*, **90**, 38 (2012).
6. F. M. A. Lino, L. Z. de Sá, I. M. S. Torres, M. L. Rocha, T. C. P. Dinis, P. C. Ghedini, V. S. Somerset and E.S. Gil, *Electrochim. Acta*, **128**, 25 (2014).
7. A. S. Arribas, M. Martínez-Fernández, M. Moreno, E. Bermejo, A. Zapardiel and M. Chicharro, *Food Chem.*, **136**, 1183 (2013).
8. S. Chawla, R. Rawal, S. Sharma and C. S. Pundir, *Biochem. Eng. J.*, **68**, 76 (2012).
9. R. Rawal, S. Chawla and C. S. Pundir, *Anal. Biochem.*, **419**, 196 (2011).
10. M. Di Fusco, C. Tortolini, D. Deriu and F. Mazzei, *Talanta*, **81**, 235 (2010).
11. J. H. Coelho, A. P. P. Eisele, C. F. Valezi, G. J. Mattos, J. G. Schirmann, R. F. H. Dekker, A.M. Barbosa-Dekker and E. R. Sartori, *Talanta*, **204**, 475 (2019).
12. Y. Zuo, J. Xu, X. Zhu, X. Duan, L. Lu and Y. Yu, *Microchim. Acta*, **186**, 171 (2019).
13. M. A. Deshmukh, R. Celiesiute, A. Ramanaviciene, M. D. Shirsat and A. Ramanavicius, *Electrochim. Acta*, **259**, 930 (2018).
14. S. I. Kaya, S. Kurbanoglu and S. A. Ozkan, *Crit. Rev. Anal. Chem.*, **49**, 101 (2019).
15. J. R. Camargo, I. A. A. Andreotti, C. Kalinke, J. M. Henrique, J. A. Bonacin and B. C. Janegitz, *Talanta*, **208**, 120458 (2020).
16. N. P. Shettia, M. M. Shanbhag, S. J Malode, R. K. Srivastava and K. Raghava Reddy, *Microchem. J.*, **153**, 104389 (2020).
17. M. Govindasamy, S. F. Wang, B. Subramanian, R. Jothi Ramalingam, H. Al-lohedan and A. Sathiyane, *Ultrason. Sonochem.*, **58**, 104622 (2019).
18. J. Yang, D. Li, J. Fu, F. Huang and Q. Wei, *J. Electroanal. Chem.*, **766**, 16 (2016).
19. M. Gamella, S. Campuzano, A. J. Reviejo and J. M. Pingarrón, *J. Agric. Food Chem.*, **54**, 7960 (2006).
20. A. I. Yaropolov, O. V. Skorobogat'ko, S. S. Vartanov and S. D. Varfolomeyev, *Appl. Biochem. Biotechnol.*, **49**, 257 (1994).
21. V. Vukojević, S. Djurdjić, M. Ognjanović, M. Fabián, A. Samphao, K. Kalcher and D. M. Stanković, *J. Electroanal. Chem.*, **8236**, 610 (2018).
22. S. Đurđić, V. Vukojević, F. Vlahović, M. Ognjanović, Ľ. Švorc, K. Kalcher, J. Mutić and D. M. Stanković, *J. Electroanal. Chem.*, **850**, 113400 (2019).
23. J. Wang, B. Tian, V. B. Nascimento and L. Angnes, *Electrochim. Acta*, **43**, 3459 (1998).
24. X. Li, W. Zhao, R. Yin, X. Huang and L. Qian, *Eng. Sci.*, **3**, 89 (2018).
25. C. Liu, M. Chen, W. Yu and Yan He, *ES Energy Environ.*, **2**, 31 (2018).
26. Y. Guo, X. Yang, K. Ruan, J. Kong, M. Dong, J. Zhang, J. Gu and Z. Guo, *ACS Appl. Mater. Interfaces*, **11**, 25465 (2019).
27. L. Qiu, P. Guo, H. Zou, Y. Feng, X. Zhang, S. Pervaiz and D. Wen, *ES Energy Environ.*, **2**, 66 (2018).
28. Y. Chen, Y. Wang, T. Su, J. Chen, C. Zhang, X. Lai, D. Jiang, Z. Wu, C. Sun, B. Li and

Z. Guo, *ES Mater. Manuf.*, **4**, 31 (2019).
29. N. Nidamanuri, Y. Li, Q. Li and M. Dong, *Eng. Sci.*, **9**, 3 (2020).
30. Y. Zhang, Y. Yan, J. Guo, T. Lu, J. Liu, J. Zhou and X. Xu, *ES Energy Environ.*, *IN PRESS*, DOI:10.30919/esee8c386 (2020).
31. J. Tan, D. Li, Y. Liu, P. Zhang, Z. Qu, Y. Yan, H. Hu, H. Cheng, J. Zhang, M. Dong, C. Wang, J. Fan, Z. Li, Z. Guo and M. Liu, *J. Mater. Chem. A*, **8**, 7980 (2020).
32. J. Cai, J. Tian, H. Gu and Z. Guo, *ES Mater. Manuf.*, **6**, 68 (2019).
33. G. Xu, L. Zhang, W. Yu, Z. Sun, J. Guan, J. Zhang, J. Lin, J. Zhou, J. Fan, V. Murugadoss and Z. Guo, *Nanotechnology*, **31**, 225402 (2020).
34. Y. Guo, G. Xu, X. Yang, K. Ruan, T. Ma, Q. Zhang, J. Gu, Y. Wu, H. Liu and Z. Guo, *J. Mater. Chem. C*, **6**, 3004 (2018).
35. M. Pumera, A. Ambrosi, A. Bonanni, E. L. K. Chng and H. L. Poh, *Trends Analyt. Chem.*, **29**, 954 (2010).
36. M. Pumera, *Chem. Soc. Rev.*, **39**, 4146 (2010).
37. H. Wu, J. Wang, X. Kang, C. Wang, D. Wang, J. Liu, I. A. Aksay and Y. Lin, *Talanta*, **80**, 403 (2009).
38. C. Lou, T. Jing, J. Zhou, J. Tian, Y. Zheng, C. Wang, Z. Zhao, J. Lin, H. Liu, C. Zhao and Z. Guo, *Int. J. Biol. Macromol.*, **149**, 1130 (2020).
39. C. Lou, T. Jing, J. Tian, Y. Zheng, J. Zhang, M. Dong, C. Wang, C. Hou, J. Fan and Z. Guo, *J. Mater. Res.*, **34**, 2964 (2019).
40. Z. Shi, X. Shi, M. W. Ullah, S. Li, V. V. Revin and G. Yang, *Adv. Compos. Hybrid Mater.*, **1**, 79 (2018).
41. H. Huang, L. Han, Y. Wang, Z. Yang, F. Zhu and M. Xu, *Eng. Sci.*, **9**, 60 (2020).
42. J. Cai, W. Xu, Y. Liu, Z. Zhu, G. Liu, W. Ding, G. Wang, H. Wang and Y. Luo, *Eng. Sci.*, **5**, 21 (2019).
43. J. Zhao, Q. Shao, S. Ge, J. Zhang, J. Lin, D. Cao, S. Wu, M. Dong and Z. Guo, *Chem. Rec.*, **20**, 1 (2020).
44. J. Chen, Q. Yu, X. Cui, M. Dong, J. Zhang, C. Wang, J. Fan, Y. Zhu and Z. Guo, *J. Mater. Chem. C*, **7**, 11710 (2019).
45. Cai Shi, H. Qi, R. Ma, Z. Sun, L. Xiao, G. Wei, Z. Huang, S. Liu, J. Li, M. Dong, J. Fan and Z. Guo, *Mater. Sci. Eng. C*, **105**, 110132 (2019).
46. V. Vukojević, S. Djurdjić, M. Ognjanović, B. Antić, K. Kalcher, J. Mutić and D. M. Stanković, *Biosens. Bioelectron.*, **117**, 392 (2018).
47. C. Shan, H. Yang, D. Han, Q. Zhang Q, A. Ivaska and L. Niu, *Biosens. Bioelectron.*, **25**, 1070 (2010).
48. C. Shan, H. Yang, J. Song, D. Han, A. Ivaska and L. Niu, *Anal. Chem.*, **81**, 2378 (2009).
49. A. A. Ensafi, P. Nasr-Esfahani and B. Rezaei, *Sens. Actuators B Chem.*, **270**, 192 (2018).
50. P. Xie, Y. Li, Q. Hou, K. Sui, C. Liu, X. Fu, J. Zhang, V. Murugadoss, J. Fan, Y. Wang, R. Fan and Z. Guo, *J. Mater. Chem. C*, **8**, 3029 (2020).
51. R. Moriche, A. Jiménez-Suárez, M. Sánchez, S. G. Prolongo and A. Ureña, *Compos. Sci. Technol.*, **146**, 59 (2017).
52. C. Lou, T. Jing, J. Zhou, J. Tian, Y. Zheng, C. Wang, Z. Zhao, J. Lin, H. Liu, C. Zhao and Z. Guo, *Int. J. Biol. Macromol.*, **149**, 1130 (2020).

53. C. Lou, T. Jing, J. Tian, Y. Zheng, J. Zhang, M. Dong, C. Wang, C. Hou, J. Fan and Z. Guo, *J. Mater. Res.*, **34**, 2964 (2019).
54. S. MansouriMajd, H. Teymourian, A. Salimi and R. Hallaj, *Electrochim. Acta*, **108**, 707 (2013).
55. X. Shi, W. Gu, B. Li, N. Chen, K. Zhao and Y. Xian, *Microchim. Acta*,**181**, 1 (2014).
56. C. Charan and V. K. Shahi, *J. Appl. Electrochem.*, **44**, 953 (2014).
57. I. Djerdj, D. Arčon, Z. Jagličić and M. Niederberger, *J. Phys. Chem. C*, **111**, 3614 (2007).
58. L. Wang, M. Deng, G. Ding, S. Chen and F. Xu, *Electrochim. Acta*, **114**, 416 (2013).
59. Y. H. Bai, Y. Du, J. J. Xu and H. Y. Chen, *Electrochem. Commun.*, **9**, 2611 (2007).
60. C. Zhang, Y. Zhang, Z. Miao, M. Ma, X. Du, J. Lin, B. Han, S. Takahashi, J. i. Anzai and Q. Chen, *Sens. Actuators B Chem.*, **222**, 663(2016).
61. X. Zhuang, D. Chen, S. Wang, H. Liu and L. Chen, *Sens. Actuators B Chem.*, **251**, 185 (2017).
62. N. M. Lugonja, D. M. Stanković, B. Miličić, S. D. Spasić, V. Marinković and M. M. Vrvić, *Food Chem.*, 240, 567 (2018).
63. A. J. Blasco, M. C. Rogerio, M. C. Gonzalez and A. Escarpa, *Anal. Chim. Acta*, **539**, 237 (2005).
64. Z. Hu, Y. Zhao, J. Liu, J. Wang, B. Zhang and X. Xiang, *J. Colloid Interface Sci.*, **483**, 26 (2016).
65. W. Yang, J. Zhang, Q. Ma, Y. Zhao, Y. Liu and H. He, *Sci. Rep.*, **7**, 4550 (2017).
66. N. Parveen, N. Mahato, M. O. Ansari and M. H. Cho, *Compos. B Eng.*, **87**, 281 (2016).
67. M. Navarreto-Lugo, J. H. Lim and A. C. S. Samia, *J. Electrochem. Soc.*, **165**, B83 (2018).
68. M. A. H. Nawaz, S. Rauf, G. Catanante, M. H. Nawaz, G. Nunes, J. L. Marty and A. Hayat, *Sensors*,**16**, 1651 (2016).
69. P. Zhu and Y. Zhao, *Mater. Chem. Phys.*, **233**, 60 (2019).
70. B. A. Kuznetsov, G. P. Shumakovich, O. V. Koroleva, A. I. Yaropolov, *Biosens. Bioelectron.*, **16**, 73 (2001).
71. S. A. S. S. Gomes, J. M. F. Nogueira and M. J. F. Rebelo, *Biosens. Bioelectron.*, **20**, 1211 (2004).
72. R. S. Freire, S. Thongngamdee, N. Durán, J. Wang and L. T. Kubota, *Analyst*, **127**, 258 (2002).
73. D. Leech and F. Daigle, *Analyst*, **123**, 1971 (1998).
74. J. J. Xu, X. L. Luo, Y. Du and H. Y. Chen, *Electrochem. Commun.*, **6**, 1169 (2004).
75. M. Bilgi and E. Ayranci, *Sens. Actuators B Chem.*, **237**, 849 (2016).
76. A. M. Othman and U. Wollenberger, *Int. J. Biol. Macromol.*, **153**, 855 (2020).
77. I. Vasilescu, S. A. V. Eremia, M. Kusko, A. Radoi, E. Vasile and G. L. Radu, *Biosens. Bioelectron.*, **75**, 232 (2016).
78. C. Lanzellotto, G. Favero, L. M. Antonelli, C. Tortolini, S. Cannistraro, E. Coppari and F. Mazzei, *Biosens. Bioelectron.*, **55**, 430 (2014).
79. Y. Liu, X. Qu, H. Guo, H. Chen, B. Liu and S. Dong, *Biosens. Bioelectron.*, **21**, 2195 (2006).
80. G. Gupta, V. Rajendran and P. Atanassov, *Electroanalysis*, **15**, 1577 (2003).
81. M. Elkaoutit, I. Naranjo-Rodriguez, K. R. Temsamani, M. Domínguez De La Vega and

J. L. Hidalgo-Hidalgo De Cisneros, *J. Agric. Food Chem.*, **55**, 8011 (2007).
82. Y. Zhang, Z. Lv, J. Zhou, Y. Fang, H. Wu, F. Xin, W. Zhang, J. Ma, N. Xu, A. He, W. Dong and M. Jiang, *Electroanalysis*, **31**, 1 (2019).
83. V. Vasić, U. Gašić, D. Stanković, D. Lušić, D. Vukić-Lušić, D. Milojković-Opsenica, Ž. Tešić and J. Trifković, *Food Chem.*, **274**, 629 (2019).
84. B. B. Petković, D. Stanković, M. Milčić, S. P. Sovilj and D. Manojlović, *Talanta*, **132**, 513 (2015).

Tables

Table 1. A comparison of the electrochemical performances of developed SPCE/GNP@MnO_2/TvL/Naf biosensor with other laccase biosensors reported in literature

Electrode	Technique	Working potential (V)	Model compound	Linear range (µmol L^{-1})	LOD (µmol L^{-1})	Sensitivity (nA/µmol L^{-1})	References
SPCE/MoS_2/GQDs/TvL	Amper.	+0.05	Caffeic acid	0.38 - 10.00	0.32	17.92 ± 0.21	[77]
SPE/MWCNTS/ThL	Amper. /FIA	-0.1	Gallic acid	0.6 - 100.0	1.7	35	[10]
GCE/TvL	Amper. /FIA	- 0.2	Caffeic acid	4 - 55	4	3.0 ± 0.2	[19]
Au-SAM/AuNPs-Lin/Fuller/TvL	Amper.	-0.1	Gallic acid	30 - 300	6	not given	[78]
GC/CNTs-CS/TvL	Amper.	-0.1	Catechol	1.2 - 30.0	0.66	not given	[79]
Ag/thiol monolayers/Laccase	Amper.	0.0	Catechol	1 - 400	not given	15	[80]
CE/Sonogel/TvL-Tyr	Amper.	-0.15	Caffeic acid	0.01 - 2.00	0.026	167.53	[81]
AgCl/Ag-Pt/mem*/Laccase	Amper.	+0.1	Catechin/Caffeic acid	2 - 14	1	0.0566	[71]
GCE/thGP@AuNP/CotA laccase	Amper.	-0.05	Hydroquinone	1.6 - 409.6	0.3	111	[82]
SPCE/GNP/MnO_2/TvL/Naf	**Amper.**	**+0.4**	**Caffeic acid**	**5 - 320**	**1.9**	**455**	***The current study***

SPCE - screen printed carbon electrode, MoS_2 - molybdenum disulfide, GODs - graphene quantum dots, TvL - *Trametes versicolor* Laccase, SPE - screen printed electrodes, MWCNTs - multi-walled carbon nanotubes, ThL – *Trametes hirsuta* Laccase, Au-SAM - gold-self-assembled monolayer, AuNPs - gold nanoparticles, Lin - Linker, Fuller - Fullerenols, GC - glassy carbon, CNTs-CS - carbon nanotubes-chitosan, Ag - silver, CE - carbon electrode, Tyr - *Tyrosinase*, AgCl - silver chloride, Pt - platinum, mem* - polyethersulphone membranes, Amper. - amperometry, FIA - flow injection analysis, thGP - thiol graphene, CotA laccase - CotA laccase from *Bacillus subtilis*.

Table 2. Polyphenolic index in wine obtained with developed SPCE/GNP@MnO_2/TvL/Naf biosensor (BPI) and glassy carbon electrode (EPI)

Sample	Standard additions♦ (µL)	BPI (mg/L)	EPI (mg/L)	Average ± SD (RSD) **BPI* (mg/L)**	**EPI* (mg/L)**	Recovery (%)
Red wine	100	1840	1895	**1897 ± 50 (2.62%)**	**1929 ± 60 (2.90%)**	98.3
	150	1923	1994			
	200	1929	1899			
White wine	100	521	529	**533 ± 10 (1.96%)**	**525 ± 9 (1.55%)**	98.5
	150	538	516			
	200	540	531			

♦ 0.005 mol L^{-1} caffeic acid

* Expressed as mg caffeic acid equivalents per L of wine

Figures

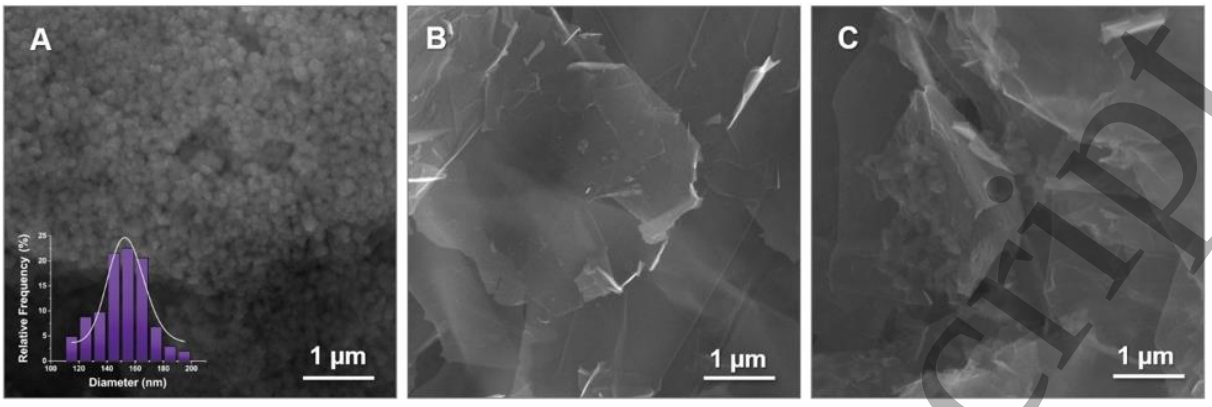

Figure 1.

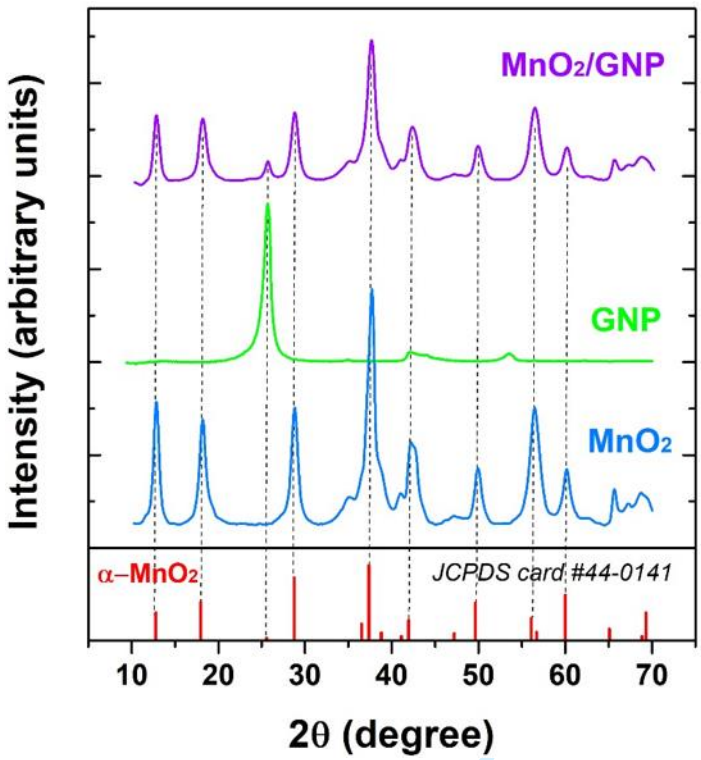

Figure 2.

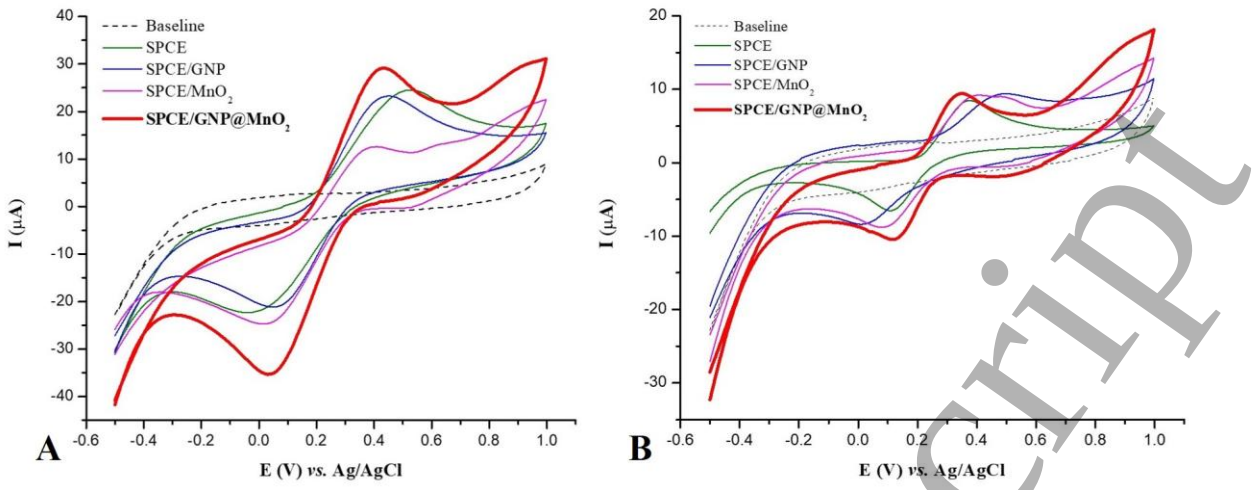

Figure 3.

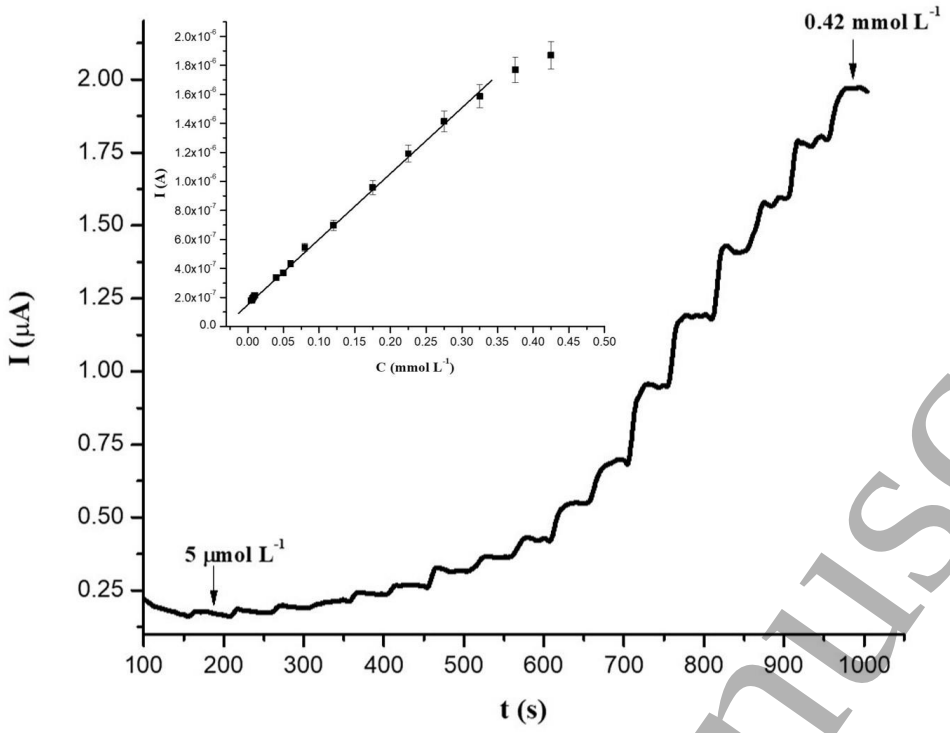

Figure 4.

Figure Captions

Figure 1. FE-SEM micrographs of (A) MnO_2 nanoparticles, (B) graphene nanoplatelets and (C) GNP@MnO_2 nanocomposite. Inset of Fig. 1A shows log-normal size distribution of MnO_2 nanoparticles.

Figure 2. XRPD patterns of the synthesized samples: MnO_2 nanoparticles *(blue line)*, GNP *(green line)*, GNP@MnO_2 nanocomposite *(purple line)*. The standard data for α-MnO_2 (JCPDS card #44-0141) were presented in the figure for comparison.

Figure 3. A) Cyclic voltammograms for A) 0.5 mmol L^{-1} $K_3[Fe(CN)_6]/K_4[Fe(CN)_6]$ and B) 0.1 mmol L^{-1} caffeic acid, recorded with unmodified SPCE and SPCE modified with GNP (SPCE/GNP), MnO_2 (SPCE/MnO_2) and GNP@MnO_2 (SPCE/GNP@MnO_2) in 0.1 mol L^{-1} PB (pH=6.50), and the scan rate of 50mV/s.

Figure 4. Constant potential (0.4 V *vs.* Ag/AgCl) amperometry of SPCE/GNP@MnO_2/TvL/Naf biosensor after successive addition of different aliquots of 5 mmol L^{-1} caffeic acid under stirring conditions. The inset in the figure represents the calibration curve with corresponding error bars for the obtained oxidation current versus the different concentrations of caffeic acid.